

Leveraging Chemistry Foundation Models to Facilitate Structure Focused Retrieval Augmented Generation in Multi-Agent Workflows for Catalyst and Materials Design

Nathaniel H. Park,^{1,*} Tiffany J. Callahan,¹ James L. Hedrick,¹ Tim Erdmann,¹ and Sara Capponi¹

¹IBM Research–Almaden, 650 Harry Rd. San Jose, CA 95120

*Corresponding author. Email: npark@us.ibm.com

Abstract

Molecular property prediction and generative design via deep learning models has been the subject of intense research given its potential to accelerate development of new, high-performance materials. More recently, these workflows have been significantly augmented with the advent of large language models (LLMs) and systems of LLM-driven agents capable of utilizing pre-trained models to make predictions in the context of more complex research tasks. While effective, there is still room for substantial improvement within the agentic systems on the retrieval of salient information for material design tasks. Moreover, alternative uses of predictive deep learning models, such as leveraging their latent representations to facilitate cross-modal retrieval augmented generation within agentic systems to enable task-specific materials design, has remained unexplored. Herein, we demonstrate that large, pre-trained chemistry foundation models can serve as a basis for enabling semantic chemistry information retrieval for both small-molecules, complex polymeric materials, and reactions. Additionally, we show the use of chemistry foundation models in conjunction with image models such as OpenCLIP facilitate unprecedented queries and information retrieval across multiple characterization data domains. Finally, we demonstrate the integration of these systems within multi-agent systems to facilitate structure and topological-based natural language queries and information retrieval for complex research tasks.

Introduction

The advent of accessible large language models (LLMs) and their respective capabilities has enabled a dramatic expansion of LLM-based workflows across the domains of chemistry and materials. These include applications of chatbots or multi-agent workflows to metal-organic frameworks,^{1,2} inorganic materials,³ automated synthesis,⁴ organic synthesis,⁵ and protein discovery.⁶ Besides the underlying language models of the agents and their respective interactions to produce a final output, the critical components of these workflows are the tools made available to individual agents. This can include access to retrosynthetic software,⁵ predictive models or computational tools,³ or writing task-specific code for automated experimentation⁴—all of which provide salient information needed by an LLM or LLM-powered agent to complete a given task. All of these are closely related to and frequently used in combination with standard retrieval augmented generation (RAG) wherein a natural-language query is run against a corpus of chunked text documents within a vector database to retrieve the most relevant documents and provide them to the LLM as part of its prompt.⁷⁻⁹ As with other types of agent tools, this approach is effective in enhancing LLM performance for answering a particular question, it does require significant

optimization of the choice of embedding model, chunk size, LLM choice and its available context window, question rephrasing, use of metadata filtering, and similarity metrics used for chunk retrieval.^{8,9,9}

In many of the agent-based workflows noted above, the tools used may utilize structural information in the form of a SMILES string or molecular formula to perform a computation or property prediction,^{6,10,11} but not directly in RAG operations focused on structural similarity. Retrieval of relevant information based on structural similarity, whether focused small-molecules, materials, or reactions, is one of the most critical tasks during any research endeavor. Therefore, enabling researchers to use natural-language accompanied by chemical language to query structure-linked information resources would provide a powerful augmentation of LLM capabilities. Achieving structure-based RAG operations necessitates a vector-based representation of a given compound or material whereby similarity queries may be conducted. While there are a significant variety of molecular fingerprints available through cheminformatics packages such as RDKit,¹² the use chemistry language foundation models is highly attractive due to their potential dual use within an agentic system as an embedding model and a predictive tool. Despite these advantages, there exist only a few reports on the utilization of deep learning models as embedding models for similarity-based searches—limited largely to organic molecules and inorganic materials.^{13,14} And while the LLM systems have been demonstrated to search APIs such as PubChem or the general internet in the performance of chemistry-focused tasks,⁵ these search interfaces do not offer the potential breadth of both query options or structural similarity features that may be possible when using a chemistry foundation model to embed structural information and with relevant metadata. Additionally, queries based on other modalities, such as images of characterization data, have largely not been evaluated within an LLM-based agentic system nor within traditional chemistry database interfaces in spite of the immense benefit such features would confer to researchers. To overcome these limitations and dramatically expand the capabilities of multi-agent systems for materials design and development tasks, we surmised that: 1) a single, high-performance chemistry foundation model could be adapted to facilitate semantic structure searches across small-molecules, polymers, and reactions; 2) such a model could be used in combination with an image embedding model to enable multimodal semantic queries; and 3) these systems can be integrated within multi-agent systems to provide richer context while performing materials design tasks.

Before building a complete semantic structure search-based RAG pipeline within multi-agent workflows, it was imperative to evaluate the effectiveness of both the latent representations generated by the chemistry language foundation models for structural similarity queries. There exist many potentially competent embedding models to support semantic structural queries. Prior work focused on the use of ChemBERTa models to enable similarity searches for functional analogues of drugs,^{14–16} however there are other potential models that could work including MolBERT,¹⁷ Mol2Vec,¹⁸ GPT-MolBERTa,¹⁹ or ChemGPT.²⁰ For our investigation, we selected MoLFormer as a baseline embedding model which has recently been shown to be highly performant across numerous benchmarks from MoleculeNet,²¹ effective at capturing molecular similarity, as well as potentially learning 3D spatial relationships from SMILES inputs.²² To evaluate structural similarity queries, we compiled a focused dataset of ~2.5M organic small-molecules using open-source data and historical data from our own work.^{23–26} The SMILES representations were canonicalized and vector embeddings were computed for each compound using MoLFormer before insertion into a Milvus vector database (see Supporting Information for more details).²⁷ Using this dataset we evaluated the ability of using MoLFomer embeddings to

facilitate retrieval of structurally similar compounds from sample queries on known organocatalysts for ring-opening polymerization (ROP) using the Milvus vector search capabilities (Fig. 1).^{28,29}

For the result of each query, several metrics relating to the structural similarity based on either MoLFormer embedding distance (cosine, Euclidean, Fig.1) or fingerprints for each compound generated using RDKit (Tanimoto, RDKit, MACC, and Dice, Fig 1). Each score represents the similarity between the result compound and the query compound. For 1,8-diazabicyclo[5.4.0]undec-7-ene (DBU) **1a**, the top result was itself followed by several closely related structural analogues based on the cosine or Euclidean similarity (Fig. 1A). Interestingly, the second rank compound **1b** was given much lower similarity scores from most fingerprint derived metrics despite differing from **1a** only in the saturation of the imine (Fig. 1A). For **2a**, an organocatalyst for ROP designed with the aid of generative AI,²⁹ we find that while the original query was not present in the dataset, most of the core functional group features—an cyclic 5-membered guanidine and an aromatic ring—based on visual inspection (Fig. 2B). As with **1a**, most of the fingerprint-based similarity metrics indicate the result compounds as highly dissimilar, with exception of MACC (Fig. 2B). Overall, these examples further substantiate prior results²² demonstrating MoLFormer embeddings do indeed capture relevant structural information and similarity despite differing substantially in several cases from fingerprint-based metrics.

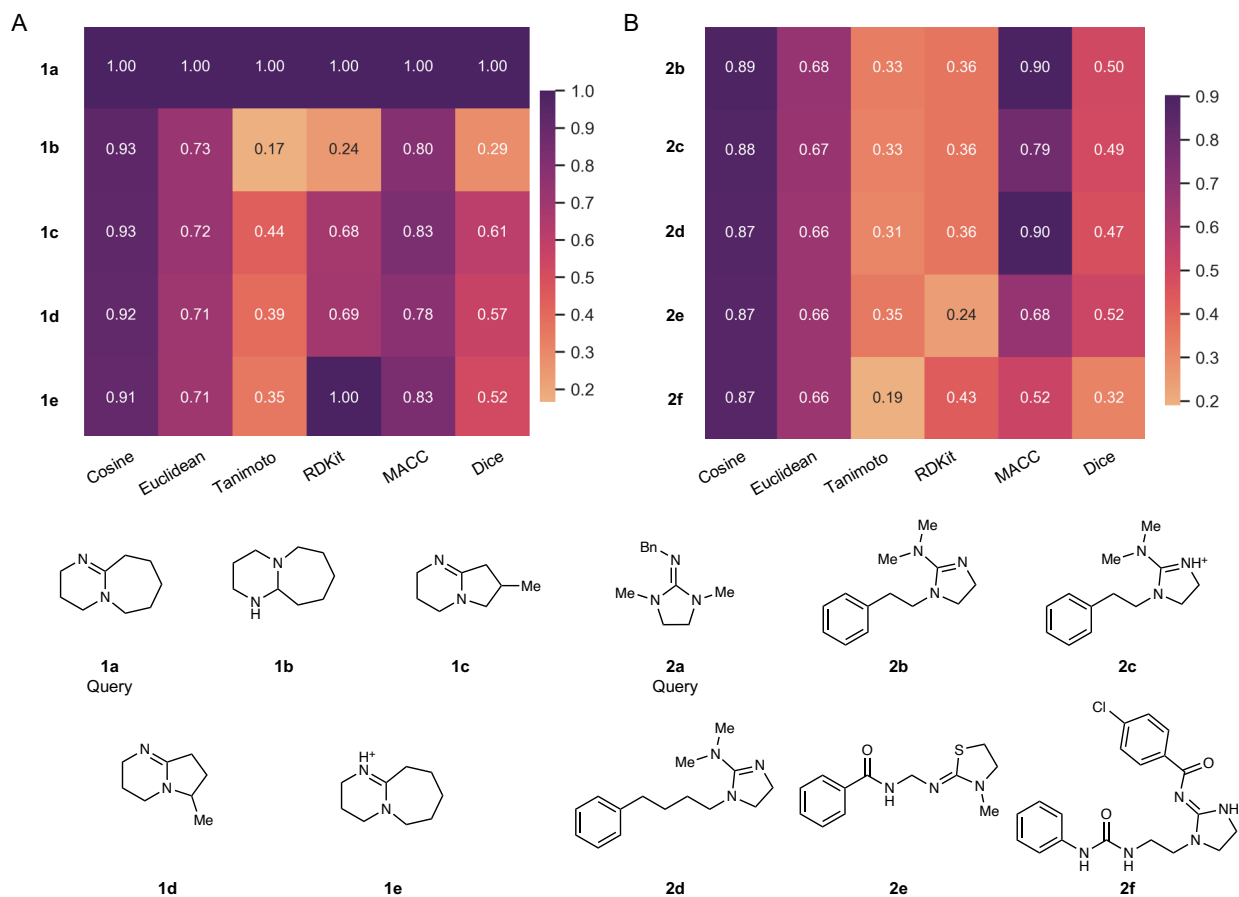


Figure 1. A) Heatmap of similarity metrics for the results of the query of **1a** against a small-molecule collection. Structures of each of the top five closest compounds are shown beneath the heatmap. B) Heatmap of similarity queries of **2a** against a small-molecule collection. Structures of each of the top five closest compounds. For the similarity metrics displayed in the heatmap, cosine and

Euclidean refer to the respective distance between the query embedding and the result embedding converted into similarity scores. Tanimoto, RDKit, MACC, and Dice refer to similarity scores from molecular fingerprints generated using the RDKit package for the query and returned compound. For all metrics, a value closer to 1 indicates high similarity whereas a value closer to zero indicates lower similarity. See Supplementary Information for details.

With the success of the similarity queries using MoLFormer embeddings in conjunction with a Milvus vector store, we sought next to expand search capabilities beyond simple small-molecule queries in order to maximize the diversity of search options available to LLM agents. In natural language, differences in word vector embeddings have been demonstrated to capture lexical relationships between different words, with classic examples of *King – Man + Woman = Queen* or *Paris – France + Poland = Warsaw* capturing the relationships of gender and capital city.³⁰ Given that MoLFormer is a chemistry language model based on SMILES syntax, we surmised differences between vector embeddings between two compounds within the base model latent space should correspond to differences in structure (Fig. 1B). Moreover, this implies that combinations of vector embeddings from compounds of interest can be used to identify novel analogues based on functional group features of both compounds as well as utilize scalar property values to manipulate the magnitude of the vector—facilitating unique similarity queries to access different sets of data. To implement these ideas, we first created an identical collection of ~2.5M molecules used in Fig. 1 where instead each vector was now scaled by the compounds' corresponding molecular weight. This was tested on guanidine **3a**, which was used as a search input to either the molecular weight scaled collection, or the base collection used previously (Fig. 2A). The results in Fig. 2A demonstrated the success of both approaches in retrieving structurally relevant compounds, however, the metadata filtering is limited to identical top results within certain molecular weight ranges (**3f**, Fig. 2A)—potentially requiring different filtering strategies depending on the desired output.

In addition to utilizing the vector magnitude to influence similarity search results, we also investigated whether addition and subtraction of vectors corresponding to different functional groups resulted in similar lexical relationships as observed with examples like: *King – Man + Woman = Queen*. This approach was evaluated on two catalysts **4a** and **4b** where their corresponding vector embeddings were subjected such operations. With **4a** the subtraction of the vector corresponding to dimethylurea and the addition of dimethylthiourea resulted in a vector embedding that provided corresponding thioureas (**4c**) when queried against the database (Fig. 2B). With **4b** the results of similar operation were less obviously successful, but this is anticipated behavior based on a limited collection of molecules (Fig. 2B). Nonetheless, the results did provide similar examples with fluorine containing amines. Finally, the vector embeddings of **4a** and **4b** were averaged and queried against the database with the top results bearing the structural features of both the parent molecules (Fig. 2C).

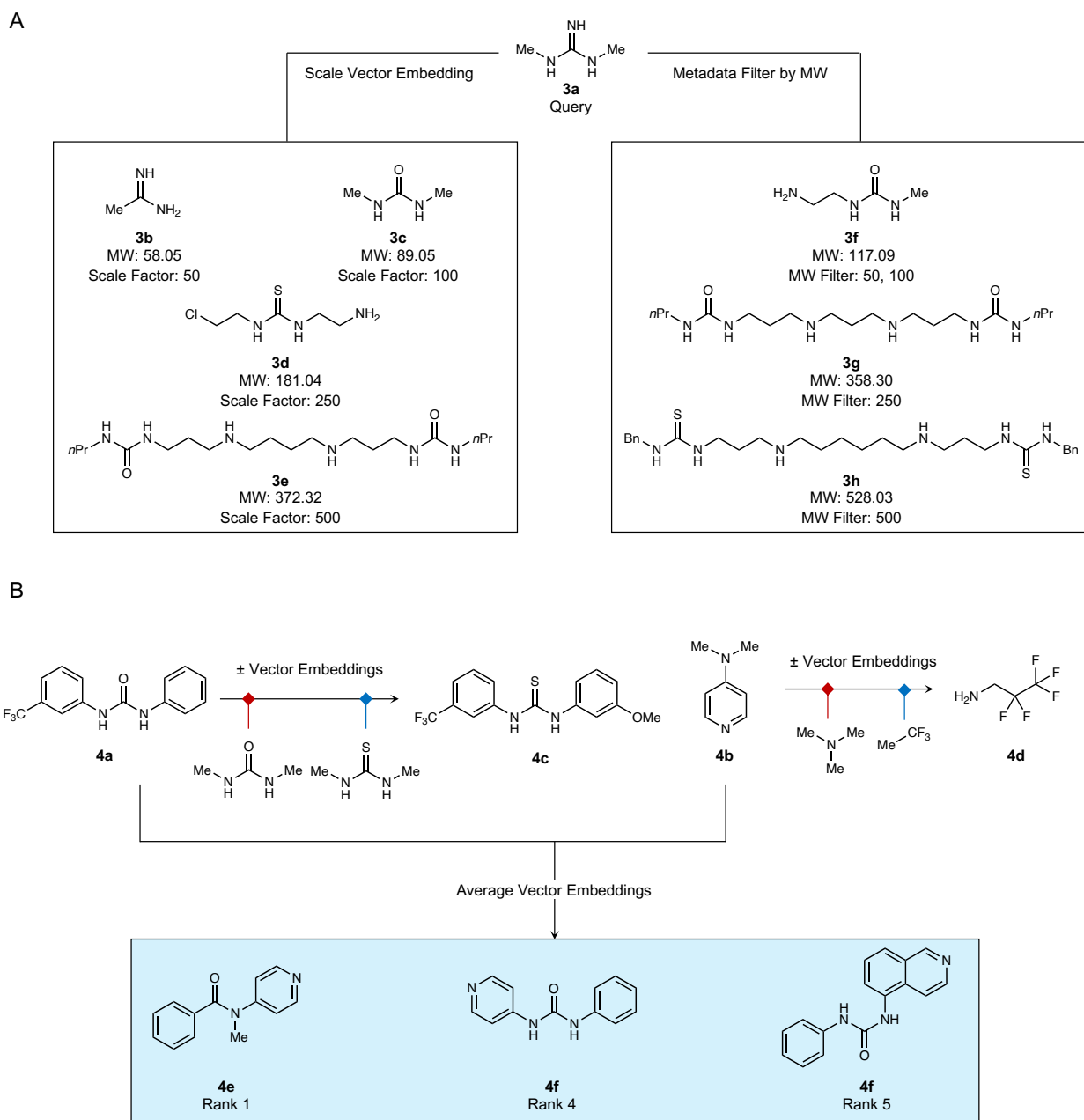


Figure 2. A) Comparison of results obtained for queries using run using metadata filters compared to normalized vector embeddings scaled by a target molecular weight. B) Schematic depiction of search results obtained through mathematical manipulation of query vector embeddings through addition-subtraction of corresponding functional group vectors or averaging two queries.

Having demonstrated the effectiveness of using MoLFormer vector embeddings on a variety of different similarity search strategies, we next sought to evaluate their feasibility towards polymers and reactions. MoLFormer was trained compounds with SMILES strings containing less than 200 tokens were filtered from the pre-training dataset, precluding large SMILES strings which may potentially represent macromolecules.²² Outside of biological materials, such as peptides, nucleic acids or large natural products, macromolecules and other complex materials are often

exhibit stochastic features relating to their structure and are hence poorly represented by discrete, one-dimensional SMILES strings. This problem is frequently circumvented in deep learning models through a reduction in the complexity by treating polymers as single, discrete repeating units via SMILES strings with variable attachment points denoted by the asterisk character.^{31,32} While this approach tends to overlook the stochastic nature of materials as well as neglecting to account for end groups or more complex polymer topologies, it does produce systems capable of providing predicted values for polymer properties within these restrictions.^{31,32} As the tokenizer for MoLFormer covers the entire SMILES grammar,^{22,33} including the use of special tokens such as variable attachment points, we hypothesized that it could also serve as a suitable source of embeddings to facilitate queries based on both polymer structural and topological similarity. It was unclear, however, as to whether these latent embeddings will capture the same level of molecular similarity given SMILES fragments with asterisks were unlikely to have been part of any pre-training set for the model. With this in mind, we leveraging dot-separated SMILES strings containing asterisks to represent repeat units or other polymer components to evaluate their suitability for use in semantic queries for polymeric materials.

To evaluate the use of MoLFormer embeddings applied to polymers, we first curated a set of polymer data from both open literature and our own historical data totaling in ~2.5M SMILES strings representing predominantly homopolymers.³⁴⁻³⁹ As with the small-molecule embeddings, these were inserted into a Milvus collection, against which similarity queries may be run. First, we tested the embeddings on very simple queries such as polyimide **5a** and polystyrene **5b**, both of which returned sets of highly similar compounds (Fig. 3A). Averaging the embeddings of **5a** and **5b** enabled the search to identify features of both, consistent with results observed on the small-molecules and again indicative of the ability of MoLFormer embeddings to capture semantic structural relationships. Next, we investigated the ability to query for two similar block copolymers **6a** and **6b**, identical in their monomer and end-group components, but differing only in block order (Fig. 3B). The spatial distance—both cosine and Euclidean—of the embedding vectors generated for each SMILES string is small, but suggestive that the model does indeed differentiate between the two. As a consequence, queries for both **6a** and **6b** give the identicals first ranked result, **6c** (Fig. 3B). It is only at the 5th ranked polymer where differences are enough to provide distinct results (**6d** and **6e**, Fig. 3B).

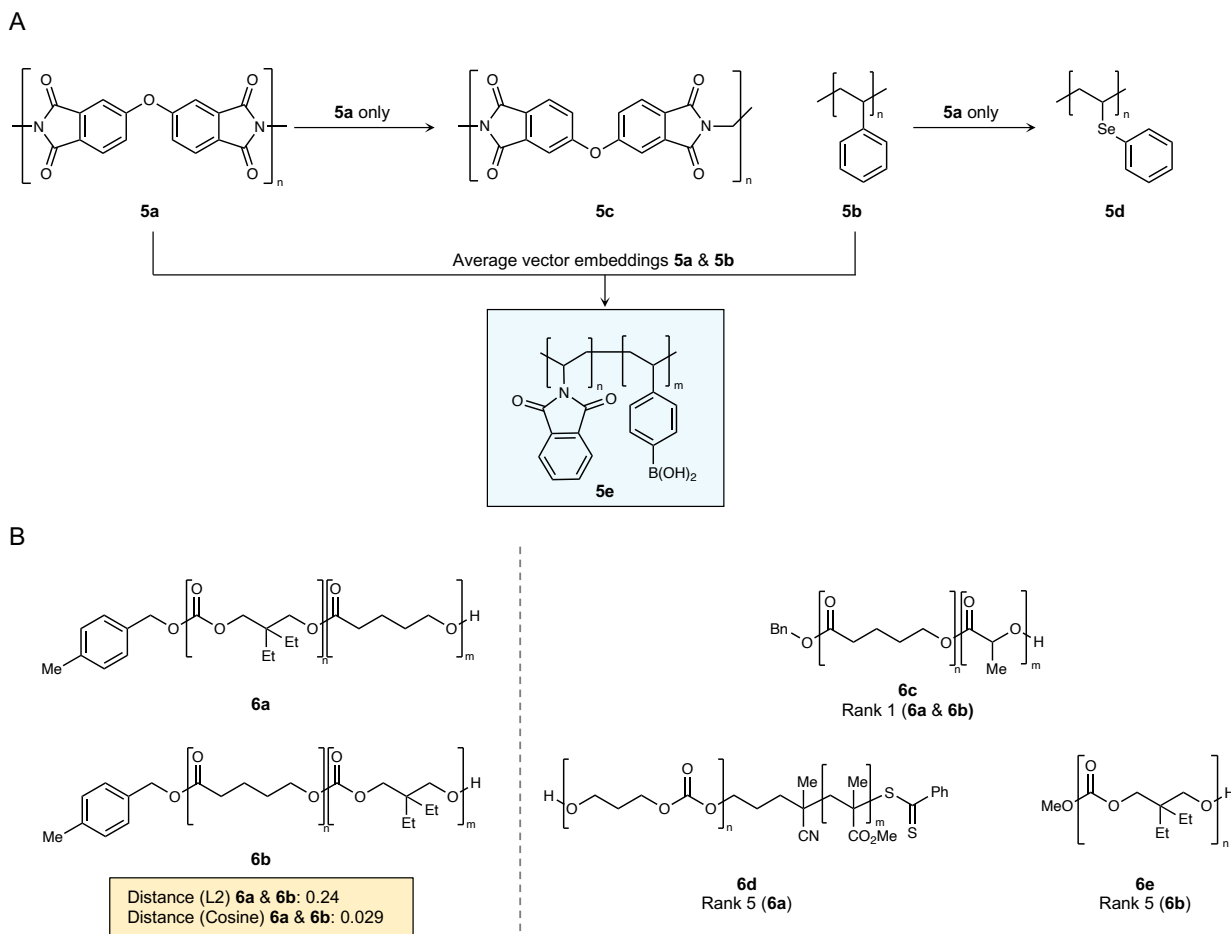
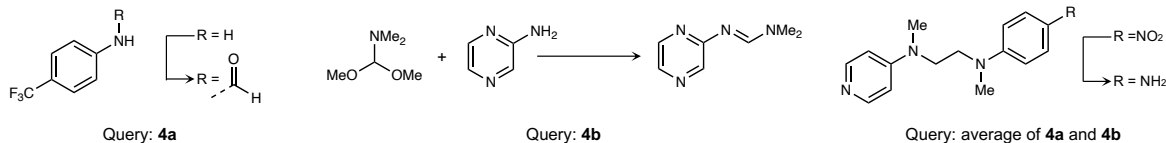


Figure 3. A) Depiction of top results for an example query for a polyimide (**5a**) and polystyrene (**5b**) for their individual MolFormer embeddings, providing results **5c** and **5d**, respectively, as well as the average of their individual embeddings providing result **5e**. The result **5d** is rank 2 as the top result of the query for **5b** was **5b**. The brackets drawn for **5e** are arbitrary, as it is unclear from the source data exactly which copolymer topology the SMILES string was intended to represent. See Supplementary Figures for full results of all queries. B). Depiction of influence of block order in co-polymers **6a** and **6b** on query results.

As with polymers, reactions—represented using reaction SMILES syntax⁴⁰—has not been examined directly using MolFormer and despite the existence of many transformer-based models for reactions,^{33,41} we were interested in probing the versatility of MolFormer embedding model reaction similarity queries. Based on our results with polymeric systems, we anticipated reactions to behave in a similar manner given a similar syntactical construction. The data for the evaluation was sourced from an open ~2M reaction dataset sourced from the USPTO used previously in transformer models for reactions, open publications, and historical experimental polymerization reaction data.⁴² In addition to querying on whole reactions, we also focused on queries involving one to two reagents (Fig. 4A). In these examples, **4a**, **4b**, and their average vector where each used to search the database and provided reaction examples where structurally related reagents were used or the query molecules themselves (Fig. 4A). Finally, testing the order of **4a** and **4b**, either in a dot separated substrate series or on either side of angle brackets (>>) separating substrates and products produced markedly different results, indicating the importance of order within the reaction SMILES sequence. The difference in results when angle brackets are used is understandable considering that this would indicate two very different reactions when the order is

reversed. However, unlike with polymers, the distinction between the ordering of reactants or products in reaction SMILES has less relevance unless some order of addition is being encoded. In total, these results indicate that the base model of MolFormer is well-suited to capture structural relationships among small-molecules, polymers, and reactions.

A



B

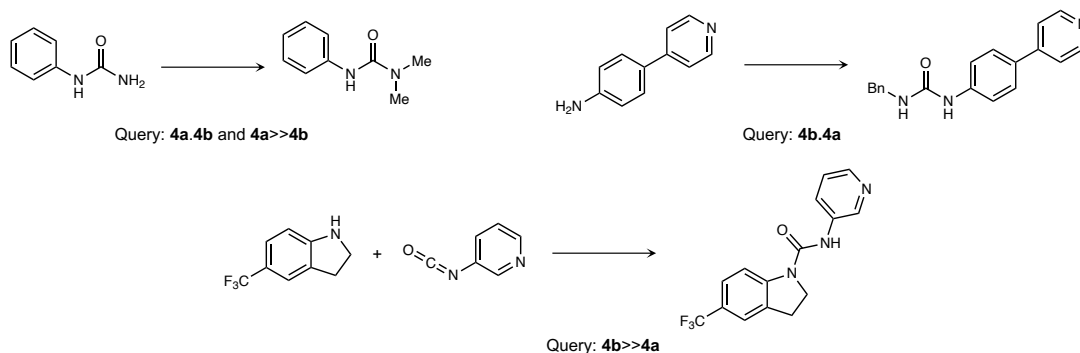


Figure 4. A) Top results of queries against 2.5 M USPTO reaction collection of embedded reaction SMILES for either **4a**, **4b**, or their average. B) Comparison of top results from concatenated query SMILES strings of **4a** and **4b** either dot separated, such as in **4a.4b**, or angle-bracket separated, such as in **4a>>4b**. Other reagents and solvents are excluded for clarity.

The demonstration of MolFormer as an effective embedding model beyond simple small molecules prompted us to examine use of chemical structural embeddings with additional modalities. Association of chemical structure with different types of characterization data is a highly important task for any project within chemistry and materials domains. While characterization data is available in many formats, we opted to leverage the data pre-plotted and saved as images as input for creation of their corresponding vector embeddings. The ability to query available characterization data by either image or structure would be a powerful addition to both traditional data infrastructures and RAG pipelines as well. To implement this task would typically require either some form contrastive learning or latent fusion, necessitating fine-tuning of an existing model or training of an additional model. Instead, we opted to test alternative strategies where the chemical components of a particular piece of characterization data would be embedded using MolFormer while the image components would be embedded using OpenCLIP image model (see Supplementary Information for details).^{43,44} While CLIP models for images can also co-embed text captions, it is not anticipated these embeddings would be able to effectively capture nuances in chemical structure as a chemistry focused model like MolFormer. Instead, the text embedder of the OpenCLIP model can be used to embed information captured as a natural language caption, which can be automatically generated from the metadata from the characterization data files, adding additional natural language query capabilities. To evaluate this approach, we compiled a small dataset of labeled images of ¹H, ¹³C, and ¹⁹F NMR spectra (see Supplementary Information). The labels for the spectra included their corresponding chemical components as SMILES strings and natural language captions generated from the spectra metadata. From this dataset we can test both image-based and structure-based queries on the embedded dataset with excellent results across numerous collection organization strategies (Fig.

5). Despite there being only minor differences between the image features plots—colors, whitespace, axes, and image size—of the embedded plots, OpenCLIP can effectively differentiate between different characterization techniques without additional metadata filtering on the query. This implies that the differentiation is likely occurring due to shape of the plotted traces or spectra (Fig. 5).

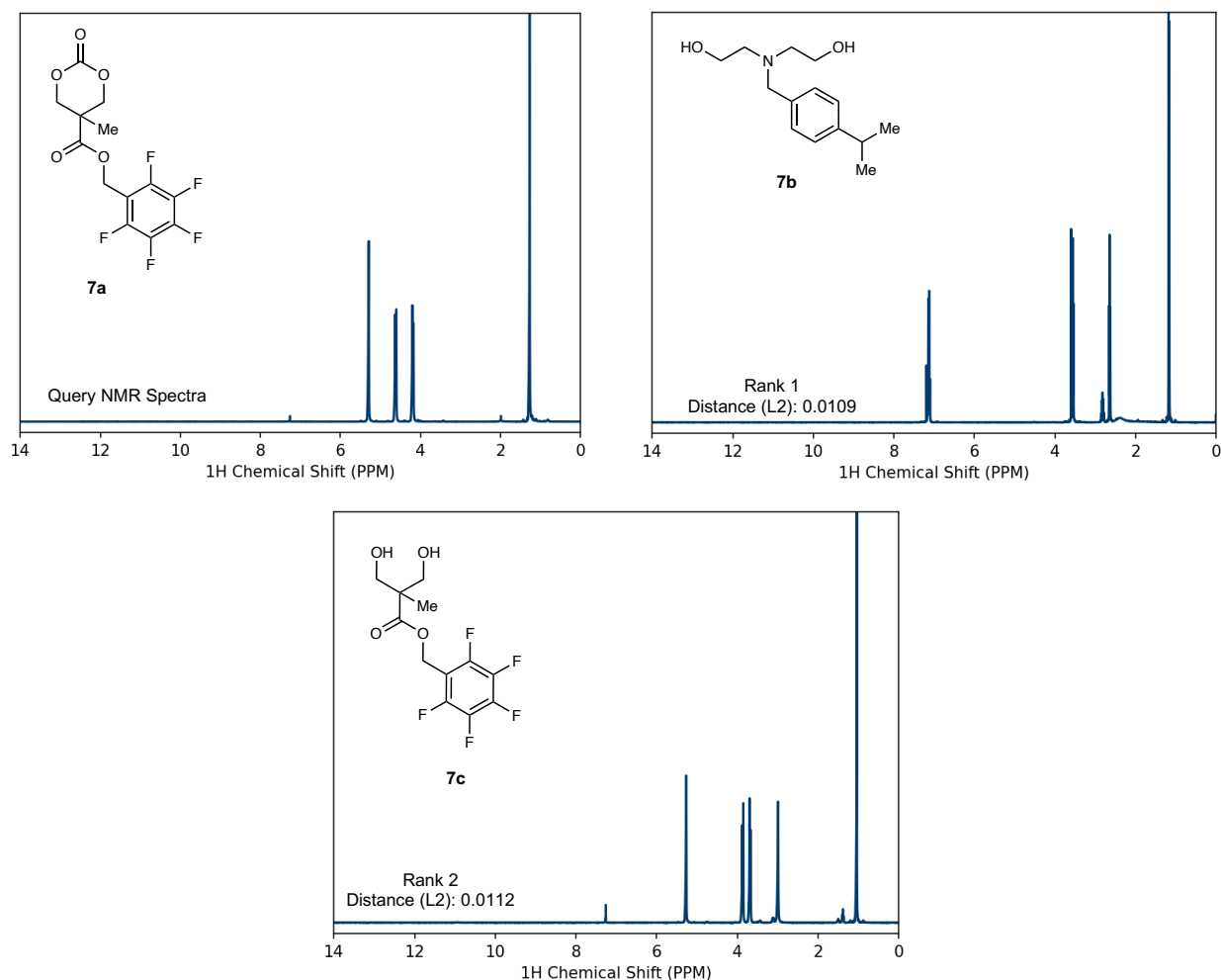


Figure 5. Example of NMR spectra similarity search using OpenCLIP image embeddings. Each spectrum is labeled with the structure of its corresponding compound. The original query is the dataset and as expected, the first result returned. Hence, the result ranks reflect those obtained after filtering out the top result.

The use of chemistry LLMs such as MoLFormer and image models like OpenCLIP, in combination with post-embedding pooling and compression strategies, has facilitated the creation of a variety of vector stores which in turn can support a large variety of similarity queries. This alone would make a powerful addition to traditional database architectures and search capabilities, yet it's the connection of such vector databases within a larger RAG framework coupled to LLM-powered agent workflows which can offer the potential of significant time savings in complex research tasks requiring the merging and summarization of data retrieved from complex structure, image, and natural language-based queries. In this regard, access to different vector stores and their respective embedding strategies is provided to LLM agents as tools which may be used in the

context of a particular task. We utilized the LangGraph library (v 0.1.19)⁴⁵ to develop a hierarchical multi-agent adaptive self-reflective RAG system (Fig. 6), which takes a question as input and outputs, the solution as a formatted research-style report. As shown in Fig. 6, the hierarchical workflow is directed by a supervisor agent which leverages query analysis⁴⁶ to adaptively route a user's question to the correct worker agent. The system consists of four worker agents, which specialize in small molecules, polymers, chemical reactions, or NMR spectra. Each of these workers autonomously implement a multi-agent-based self-reflective RAG workflow based off of.⁴⁷ As detailed in Fig. 6, the workflow consists of several steps including retrieving and evaluating documents, generating responses using retrieved documents, revising user input to improve retrieved documents, checking generated responses for hallucinations and verifying each response completely addresses a user's question. Each step of this process is autonomously directed by the worker agents, which runs until all checks are passed. Once all checks are passed, the answer is sent to the report generation tool, which summarizes the agent's findings (Figs 7-8). This report also summarizes the vector store retrieved content used by the agent to generate the report in order to improve the overall transparency of the workflow.

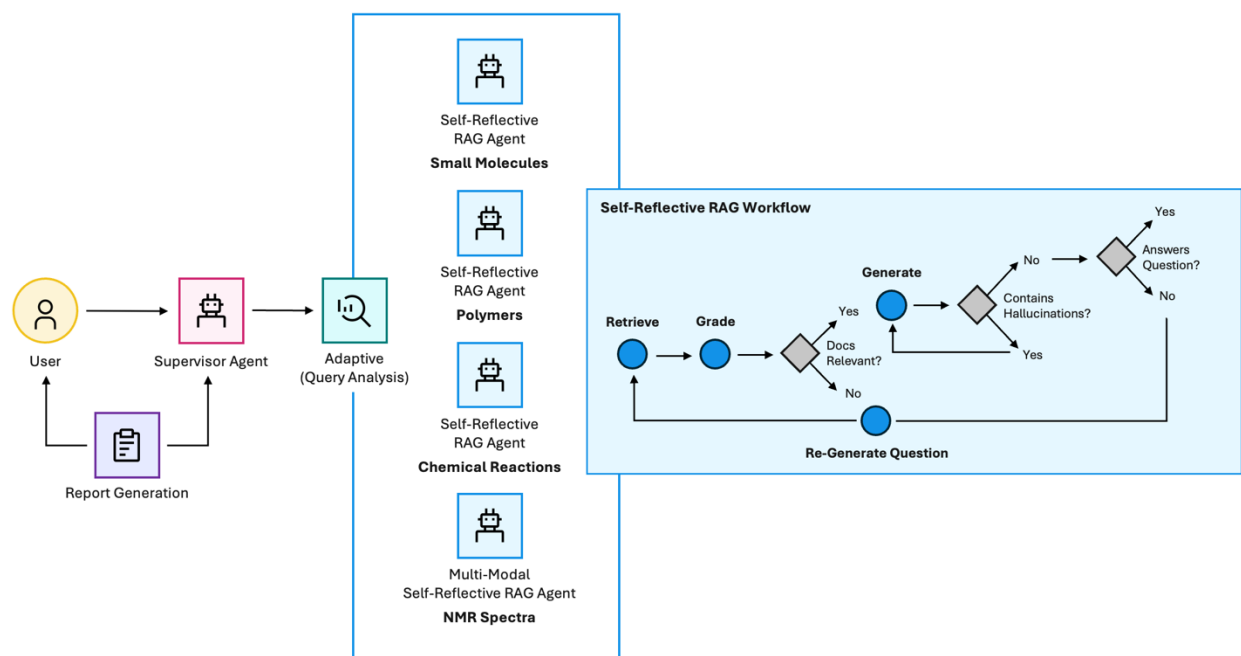


Figure 6. Overview of the Hierarchical Multi-Agent RAG System. An adaptive supervisor agent leverages query analysis to select the correct self-reflective RAG worker agent given a user query. Each self-reflective multi-agent worker autonomously performs the following tasks: (1) retrieves documents from a vector store; (2) evaluates the relevance of each retrieved document. If all documents are found to be irrelevant, a new set of documents is retrieved; (3) generates a response to the input using relevant retrieved documents; (4) inspects the generated response for hallucinations. If a response contains hallucinations, a new response is generated, and (5) determines whether the response fully addresses the user's question. If the response does not fully answer a user's question, an alternative version of the user's question is generated, and the process begins again. When all tasks are successfully completed, a response is sent to the report generation tool, which summarizes the answer to the user's question. Self-reflective RAG workflow adapted in part from Langgraph documentation.⁴⁸

This workflow was demonstrated on a variety of tasks, each of which was able to effectively utilize the structure and/or image-based vector store tools in combination with other natural language-based vector databases from historical manuscripts. Example reports generated

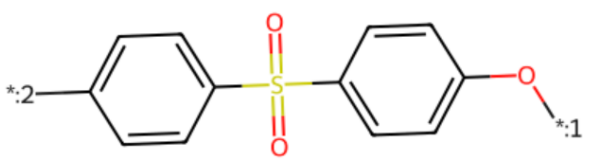
from these tasks are shown in Fig. 7 and Fig. 8 below. For Fig. 7, the agentic system was provided the following query:

“I am interested in aromatic polyethers similar in structure and function to $O=S(C1=CC=C(O[:1])C=C1)(C2=CC=C[*:2])C=C2)=O$. Please find analogues and comment on potential means of synthesis and thermal properties.”*

INTRODUCTION

The user is interested in finding analogues of a specific aromatic polyether and exploring potential synthesis methods and thermal properties.
The user's exact query was: 'I am interested in aromatic polyethers similar in structure and function to $O=S(C1=CC=C(O[*:1])C=C1)(C2=CC=C[*:2])C=C2)=O$. Please find analogues and comment on potential means of synthesis and thermal properties.'

Input Compound: $O=S(C1=CC=C(O[*:1])C=C1)(C2=CC=C[*:2])C=C2)=O$



RESEARCH STEPS

I utilized the polymer_rag_search tool to identify aromatic polyethers similar in structure and function to the provided SMILES string. The tool returned two relevant SMILES strings that represent potential analogues.

MAIN FINDINGS

The identified analogues are:

- $[*:1]c1ccc2c(c1)S(=O)(=O)c1cc([*:2])ccc1-2$
- $[*:1]c1cc(S(=O)(=O)C(F)(F)F)cc([*:2])c1C$

These structures feature sulfur-oxygen bonds and aromatic rings, similar to the original compound. For synthesis, aromatic polyethers can typically be synthesized through nucleophilic substitution reactions or using organocatalysts for polymerization. The thermal properties of these compounds can vary based on their specific structures and substituents, but generally, aromatic polyethers exhibit good thermal stability due to the strength of the aromatic bonds.

CONCLUSION

In summary, two potential analogues of the specified aromatic polyether have been identified, along with general methods for their synthesis and considerations regarding their thermal properties.

SOURCES

- polymer_rag_search tool for identifying analogues and synthesis methods.

****Summary of Vector Store Context:****
Compound(s):
- $[*:1]c1cc(S(=O)(=O)C(F)(F)F)cc([*:2])c1C$

Figure 7. Example of a report generated for a question routed to the self-reflective RAG agent for polymers.

As shown in Fig. 7, the agent was able to successfully complete the user query using the self-reflective RAG agent for polymers returning two relevant, similar analogs and provided additional content to justify the selection of these analogs stating:

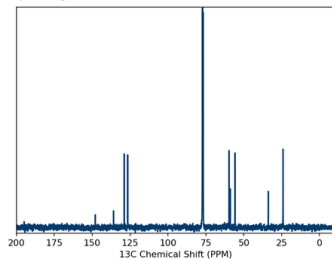
“These structures feature sulfur-oxygen bonds and aromatic rings, similar to the original compound. For synthesis, aromatic polyethers can typically be synthesized through nucleophilic substitution reactions or using organocatalysts for polymerization. The thermal properties of these compounds can vary based on their specific structures and substituents, but generally, aromatic polyethers exhibit good thermal stability due to the strength of the aromatic bonds.”

For Fig. 8, the agentic system was asked to identify similar ^{13}C NMR spectra to the one of a diethanolamine-based carbonate monomer precursor.⁴⁹ As Fig. 6, the question was routed to the multi-modal NMR agent who reviewed and summarized the characterization data of four ^{13}C NMR spectra images (i.e., three retrieved images and the image corresponding to the input) summarizing the location of the peaks in these images that similar to the input NMR spectra. The report also provides a visualization of the input image, which makes enables easier review and interpretation of the provided results. Both reports were reviewed by a domain expert confirmed who confirmed the validity of the findings. In this example, the agent was not instructed to filter the RAG results if they contained the original query, yet it still successfully found several spectra of closely related diethanolamine-based cyclic carbonates or their precursors.

INTRODUCTION

The user requested identification of NMR spectroscopy images and characterization data for compounds similar to those depicted in a provided image. The user's exact query was: 'Please identify NMR spectroscopy images along with characterization data for compounds that are similar to those depicted in the provided image. data/images/NMR/83a-13C/83a-1.png'.

Input Image:



RESEARCH STEPS

I utilized the nmr_image_rag_search tool to analyze the provided image and retrieve relevant NMR spectra and characterization data for similar compounds.

MAIN FINDINGS

The analysis yielded several NMR spectra and their corresponding peaks for compounds similar to those depicted in the provided image. The compounds include:

1. **C(C)Clccc(O(N(CCO)CCO)c1** - Peaks (ppm): 148.0, 135.9, 128.9, 126.6, 77.4, 77.0, 76.7, 59.6, 58.9, 55.7, 33.8, 24.0.
2. **C1ccc(C)cc(O(N(CCO)CCO)c1** - Peaks (ppm): 138.6, 138.0, 129.0, 126.8, 77.4, 77.0, 76.7, 59.6, 59.1, 55.8, 21.3.
3. **C1cc(C)C(O(N2CCOC(=O)OC2)c(C)C1** - Peaks (ppm): 138.2, 137.1, 130.8, 129.2, 77.9, 77.8, 77.7, 77.6, 77.4, 77.0, 76.7, 69.8, 54.7, 53.8, 20.9, 20.0.
4. **OCCN(CCO)C1c2ccccc2-c2ccccc21** - Peaks (ppm): 144.4, 140.8, 128.4, 127.4, 125.2, 128.1, 78.1, 77.7, 77.4, 77.0, 76.7, 67.8, 60.5, 54.1.

CONCLUSION

The retrieved NMR spectra and characterization data provide valuable insights into compounds similar to those depicted in the provided image, highlighting their structural features and chemical environments.

SOURCES

- NMR spectra and characterization data retrieved from the nmr_image_rag_search tool.

Summary of Vector Store Context:

Compound(s):

- Cc1ccc(C)cc(O(N(CCO)CCO)c1;Cl(C)Cl)Cl
- Cc1ccc(C)C(O(N2CCOC(=O)OC2)c(C)C1;Cl(C)Cl)Cl
- OCCN(CCO)C1c2ccccc2-c2ccccc21;Cl(C)Cl

The NMR Spectra of the most relevant compound is shown below (data/images/NMR/83b-13C/83b-1.png):

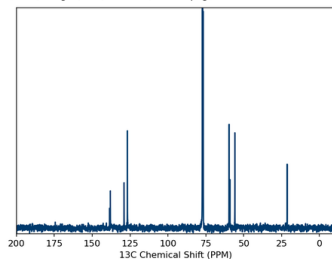


Figure Caption: A 100.62 MHz ¹³C NMR in CDCl₃ collected on 2021-02-02T14:25:28 with 256 scans and a scan delay of 4 seconds. The displayed spectrum is between 0 and 12 PPM. Peaks (ppm): 138.6, 138.0, 129.0, 126.8, 77.4, 77.0, 76.7, 59.6, 59.1, 55.8, 21.3

Figure 8. Example of a report generated for a question routed to the multi-modal self-reflective RAG agent for NMR spectra.

Conclusion

The accelerated development of novel materials and catalysts necessitates dramatic improvement of human-AI interactions to facilitate both effective co-designs as well as realistic implementations within an experimental setting. LLM-based multiagent systems integrated with chat interfaces hold significant promise to become useful assistants for researchers operating in laboratory settings. Here, we have demonstrated that chemical foundation models coupled with powerful image recognition models can facilitate unique types of multimodal structural or architectural focused queries on small-molecules, polymers, and reactions. This represents a significant enhancement of search capabilities not typically found in traditional database systems for chemistry research. Moreover, the coupling of these systems within a LLM-based multiagent system can provide a significant advantage for reducing the time needed to retrieve and summarize

relevant multimodal structure-based information commonly required across all material research projects.

Code and Data Availability

Data and code will be made available upon final publication.

Conflict of Interest

A patent application on aspects of multimodal semantic search for materials has been filed by IBM (application number 18/798970, inventors: N.H.P, T.E., and J.L.H). All authors are employees of IBM.

References

- (1) Zheng, Z.; Zhang, O.; Borgs, C.; Chayes, J. T.; Yaghi, O. M. ChatGPT Chemistry Assistant for Text Mining and the Prediction of MOF Synthesis. *J. Am. Chem. Soc.* **2023**, *145* (32), 18048–18062. <https://doi.org/10.1021/jacs.3c05819>.
- (2) Kang, Y.; Kim, J. ChatMOF: An Artificial Intelligence System for Predicting and Generating Metal-Organic Frameworks Using Large Language Models. *Nat. Commun.* **2024**, *15* (1), 4705. <https://doi.org/10.1038/s41467-024-48998-4>.
- (3) Chiang, Y.; Hsieh, E.; Chou, C.-H.; Riebesell, J. LLaMP: Large Language Model Made Powerful for High-Fidelity Materials Knowledge Retrieval and Distillation. arXiv June 2, 2024. <https://doi.org/10.48550/arXiv.2401.17244>.
- (4) Boiko, D. A.; MacKnight, R.; Kline, B.; Gomes, G. Autonomous Chemical Research with Large Language Models. *Nature* **2023**, *624* (7992), 570–578. <https://doi.org/10.1038/s41586-023-06792-0>.
- (5) Bran, A.; Cox, S.; Schilter, O.; Baldassari, C.; White, A. D.; Schwaller, P. Augmenting Large Language Models with Chemistry Tools. *Nat. Mach. Intell.* **2024**, *6* (5), 525–535. <https://doi.org/10.1038/s42256-024-00832-8>.
- (6) Ghafarollahi, A.; J. Buehler, M. ProtAgents: Protein Discovery via Large Language Model Multi-Agent Collaborations Combining Physics and Machine Learning. *Digit. Discov.* **2024**, *3* (7), 1389–1409. <https://doi.org/10.1039/D4DD00013G>.
- (7) Li, H.; Su, Y.; Cai, D.; Wang, Y.; Liu, L. *A Survey on Retrieval-Augmented Text Generation*. arXiv.org. <https://arxiv.org/abs/2202.01110v2> (accessed 2024-08-16).
- (8) Lewis, P.; Perez, E.; Piktus, A.; Petroni, F.; Karpukhin, V.; Goyal, N.; Küttler, H.; Lewis, M.; Yih, W.; Rocktäschel, T.; Riedel, S.; Kiela, D. Retrieval-Augmented Generation for Knowledge-Intensive NLP Tasks. arXiv April 12, 2021. <https://doi.org/10.48550/arXiv.2005.11401>.
- (9) Zhao, P.; Zhang, H.; Yu, Q.; Wang, Z.; Geng, Y.; Fu, F.; Yang, L.; Zhang, W.; Jiang, J.; Cui, B. Retrieval-Augmented Generation for AI-Generated Content: A Survey. arXiv June 21, 2024. <https://doi.org/10.48550/arXiv.2402.19473>.
- (10) Buehler, M. J. Generative Retrieval-Augmented Ontologic Graph and Multiagent Strategies for Interpretive Large Language Model-Based Materials Design. *ACS Eng. Au* **2024**, *4* (2), 241–277. <https://doi.org/10.1021/acsenengineeringau.3c00058>.

- (11) Ghafarollahi, A.; Buehler, M. J. AtomAgents: Alloy Design and Discovery through Physics-Aware Multi-Modal Multi-Agent Artificial Intelligence. arXiv July 13, 2024. <https://doi.org/10.48550/arXiv.2407.10022>.
- (12) Boldini, D.; Ballabio, D.; Consonni, V.; Todeschini, R.; Grisoni, F.; Sieber, S. A. Effectiveness of Molecular Fingerprints for Exploring the Chemical Space of Natural Products. *J. Cheminformatics* **2024**, *16* (1), 35. <https://doi.org/10.1186/s13321-024-00830-3>.
- (13) Yang, Y.; Liu, M.; Kitchin, J. R. Neural Network Embeddings Based Similarity Search Method for Atomistic Systems. *Digit. Discov.* **2022**, *1* (5), 636–644. <https://doi.org/10.1039/D2DD00055E>.
- (14) Kosonocky, C. W.; Feller, A. L.; Wilke, C. O.; Ellington, A. D. Using Alternative SMILES Representations to Identify Novel Functional Analogues in Chemical Similarity Vector Searches. *Patterns* **2023**, *4* (12), 100865. <https://doi.org/10.1016/j.patter.2023.100865>.
- (15) Chithrananda, S.; Grand, G.; Ramsundar, B. ChemBERTa: Large-Scale Self-Supervised Pretraining for Molecular Property Prediction. arXiv October 23, 2020. <https://doi.org/10.48550/arXiv.2010.09885>.
- (16) Ahmad, W.; Simon, E.; Chithrananda, S.; Grand, G.; Ramsundar, B. ChemBERTa-2: Towards Chemical Foundation Models. arXiv September 4, 2022. <https://doi.org/10.48550/arXiv.2209.01712>.
- (17) Li, J.; Jiang, X. Mol-BERT: An Effective Molecular Representation with BERT for Molecular Property Prediction. *Wirel. Commun. Mob. Comput.* **2021**, *2021* (1), 7181815. <https://doi.org/10.1155/2021/7181815>.
- (18) Jaeger, S.; Fulle, S.; Turk, S. Mol2vec: Unsupervised Machine Learning Approach with Chemical Intuition. *J. Chem. Inf. Model.* **2018**, *58* (1), 27–35. <https://doi.org/10.1021/acs.jcim.7b00616>.
- (19) Balaji, S.; Magar, R.; Jadhav, Y.; Farimani, A. B. GPT-MolBERTa: GPT Molecular Features Language Model for Molecular Property Prediction. arXiv October 10, 2023. <https://doi.org/10.48550/arXiv.2310.03030>.
- (20) Frey, N. C.; Soklaski, R.; Axelrod, S.; Samsi, S.; Gómez-Bombarelli, R.; Coley, C. W.; Gadepally, V. Neural Scaling of Deep Chemical Models. *Nat. Mach. Intell.* **2023**, *5* (11), 1297–1305. <https://doi.org/10.1038/s42256-023-00740-3>.
- (21) Wu, Z.; Ramsundar, B.; Feinberg, E. N.; Gomes, J.; Geniesse, C.; Pappu, A. S.; Leswing, K.; Pande, V. MoleculeNet: A Benchmark for Molecular Machine Learning. *Chem. Sci.* **2018**, *9* (2), 513–530. <https://doi.org/10.1039/C7SC02664A>.
- (22) Ross, J.; Belgodere, B.; Chenthamarakshan, V.; Padhi, I.; Mroueh, Y.; Das, P. Large-Scale Chemical Language Representations Capture Molecular Structure and Properties. *Nat. Mach. Intell.* **2022**, *4* (12), 1256–1264. <https://doi.org/10.1038/s42256-022-00580-7>.
- (23) Gallarati, S.; Gerwen, P. van; Laplaza, R.; Vela, S.; Fabrizio, A.; Corminboeuf, C. OSCAR: An Extensive Repository of Chemically and Functionally Diverse Organocatalysts. *Chem. Sci.* **2022**, *13* (46), 13782–13794. <https://doi.org/10.1039/D2SC04251G>.
- (24) Haas, B.; Hardy, M.; V, S. S. S.; Adams, K.; Coley, C.; Paton, R.; Sigman, M. Rapid Prediction of Conformationally-Dependent DFT-Level Descriptors Using Graph Neural Networks for Carboxylic Acids and Alkyl Amines. ChemRxiv February 23, 2024. <https://doi.org/10.26434/chemrxiv-2024-m5bpn>.
- (25) Zheng, J. IUPAC/Dissociation-Constants: V1.0, 2022. <https://doi.org/10.5281/zenodo.7236453>.

- (26) Wu, J.; Wan, Y.; Wu, Z.; Zhang, S.; Cao, D.; Hsieh, C.-Y.; Hou, T. MF-SuP-pKa: Multi-Fidelity Modeling with Subgraph Pooling Mechanism for pKa Prediction. *Acta Pharm. Sin. B* **2023**, *13* (6), 2572–2584. <https://doi.org/10.1016/j.apsb.2022.11.010>.
- (27) Wang, J.; Yi, X.; Guo, R.; Jin, H.; Xu, P.; Li, S.; Wang, X.; Guo, X.; Li, C.; Xu, X.; Yu, K.; Yuan, Y.; Zou, Y.; Long, J.; Cai, Y.; Li, Z.; Zhang, Z.; Mo, Y.; Gu, J.; Jiang, R.; Wei, Y.; Xie, C. Milvus: A Purpose-Built Vector Data Management System. In *Proceedings of the 2021 International Conference on Management of Data; SIGMOD '21*; Association for Computing Machinery: New York, NY, USA, 2021; pp 2614–2627. <https://doi.org/10.1145/3448016.3457550>.
- (28) Kiesewetter, M. K.; Shin, E. J.; Hedrick, J. L.; Waymouth, R. M. Organocatalysis: Opportunities and Challenges for Polymer Synthesis. *Macromolecules* **2010**, *43* (5), 2093–2107. <https://doi.org/10.1021/ma9025948>.
- (29) Park, N. H.; Manica, M.; Born, J.; Hedrick, J. L.; Erdmann, T.; Zubarev, D. Y.; Adell-Mill, N.; Arrechea, P. L. Artificial Intelligence Driven Design of Catalysts and Materials for Ring Opening Polymerization Using a Domain-Specific Language. *Nat. Commun.* **2023**, *14* (1), 3686. <https://doi.org/10.1038/s41467-023-39396-3>.
- (30) Vylomova, E.; Rimell, L.; Cohn, T.; Baldwin, T. Take and Took, Gaggles and Gooses, Book and Read: Evaluating the Utility of Vector Differences for Lexical Relation Learning. arXiv August 13, 2016. <https://doi.org/10.48550/arXiv.1509.01692>.
- (31) Xu, C.; Wang, Y.; Barati Farimani, A. TransPolymer: A Transformer-Based Language Model for Polymer Property Predictions. *Npj Comput. Mater.* **2023**, *9* (1), 1–14. <https://doi.org/10.1038/s41524-023-01016-5>.
- (32) Kuenneth, C.; Ramprasad, R. polyBERT: A Chemical Language Model to Enable Fully Machine-Driven Ultrafast Polymer Informatics. *Nat. Commun.* **2023**, *14* (1), 4099. <https://doi.org/10.1038/s41467-023-39868-6>.
- (33) Schwaller, P.; Laino, T.; Gaudin, T.; Bolgar, P.; Hunter, C. A.; Bekas, C.; Lee, A. A. Molecular Transformer: A Model for Uncertainty-Calibrated Chemical Reaction Prediction. *ACS Cent. Sci.* **2019**, *5* (9), 1572–1583. <https://doi.org/10.1021/acscentsci.9b00576>.
- (34) Ma, R.; Luo, T. PIIM: A Benchmark Database for Polymer Informatics. *J. Chem. Inf. Model.* **2020**, *60* (10), 4684–4690. <https://doi.org/10.1021/acs.jcim.0c00726>.
- (35) Aldeghi, M.; W. Coley, C. A Graph Representation of Molecular Ensembles for Polymer Property Prediction. *Chem. Sci.* **2022**, *13* (35), 10486–10498. <https://doi.org/10.1039/D2SC02839E>.
- (36) Volgin, I. V.; Batyr, P. A.; Matseevich, A. V.; Dobrovskiy, A. Yu.; Andreeva, M. V.; Nazarychev, V. M.; Larin, S. V.; Goikhman, M. Ya.; Vizilter, Y. V.; Askadskii, A. A.; Lyulin, S. V. Machine Learning with Enormous “Synthetic” Data Sets: Predicting Glass Transition Temperature of Polyimides Using Graph Convolutional Neural Networks. *ACS Omega* **2022**, *7* (48), 43678–43691. <https://doi.org/10.1021/acsomega.2c04649>.
- (37) Hu, J.; Li, Z.; Lin, J.; Zhang, L. Prediction and Interpretability of Glass Transition Temperature of Homopolymers by Data-Augmented Graph Convolutional Neural Networks. *ACS Appl. Mater. Interfaces* **2023**, *15* (46), 54006–54017. <https://doi.org/10.1021/acsami.3c13698>.
- (38) Yang, J.; Tao, L.; He, J.; McCutcheon, J. R.; Li, Y. Machine Learning Enables Interpretable Discovery of Innovative Polymers for Gas Separation Membranes. *Sci. Adv.* **2022**, *8* (29), eabn9545. <https://doi.org/10.1126/sciadv.abn9545>.

- (39) Ohno, M.; Hayashi, Y.; Zhang, Q.; Kaneko, Y.; Yoshida, R. SMiPoly: Generation of a Synthesizable Polymer Virtual Library Using Rule-Based Polymerization Reactions. *J. Chem. Inf. Model.* **2023**, *63* (17), 5539–5548. <https://doi.org/10.1021/acs.jcim.3c00329>.
- (40) *Daylight Theory: SMILES*.
<https://www.daylight.com/dayhtml/doc/theory/theory.smiles.html> (accessed 2024-08-21).
- (41) Bran, A. M.; Schwaller, P. Transformers and Large Language Models for Chemistry and Drug Discovery. arXiv October 9, 2023. <https://doi.org/10.48550/arXiv.2310.06083>.
- (42) Schwaller, P.; Probst, D.; Vaucher, A. C.; Nair, V. H.; Kreutter, D.; Laino, T.; Reymond, J.-L. Mapping the Space of Chemical Reactions Using Attention-Based Neural Networks. *Nat. Mach. Intell.* **2021**, *3* (2), 144–152. <https://doi.org/10.1038/s42256-020-00284-w>.
- (43) Ilharco, G.; Wortsman, M.; Carlini, N.; Taori, R.; Dave, A.; Shankar, V.; Namkoong, H.; Miller, J.; Hajishirzi, H.; Farhadi, A.; Schmidt, L. OpenCLIP, 2021.
<https://doi.org/10.5281/zenodo.5143773>.
- (44) Radford, A.; Kim, J. W.; Hallacy, C.; Ramesh, A.; Goh, G.; Agarwal, S.; Sastry, G.; Askell, A.; Mishkin, P.; Clark, J.; Krueger, G.; Sutskever, I. Learning Transferable Visual Models From Natural Language Supervision. In *Proceedings of the 38th International Conference on Machine Learning*; PMLR, 2021; pp 8748–8763.
- (45) Langchain-Ai/Langgraph, 2024. <https://github.com/langchain-ai/langgraph> (accessed 2024-08-21).
- (46) Jeong, S.; Baek, J.; Cho, S.; Hwang, S. J.; Park, J. C. Adaptive-RAG: Learning to Adapt Retrieval-Augmented Large Language Models through Question Complexity. arXiv March 28, 2024. <https://doi.org/10.48550/arXiv.2403.14403>.
- (47) Asai, A.; Wu, Z.; Wang, Y.; Sil, A.; Hajishirzi, H. Self-RAG: Learning to Retrieve, Generate, and Critique through Self-Reflection. arXiv October 17, 2023.
<https://doi.org/10.48550/arXiv.2310.11511>.
- (48) *langgraph/examples/rag/langgraph_crag_local.ipynb at main · langchain-ai/langgraph*. GitHub. https://github.com/langchain-ai/langgraph/blob/main/examples/rag/langgraph_crag_local.ipynb (accessed 2024-08-21).
- (49) Hedrick, J. L.; Piunova, V.; Park, N. H.; Erdmann, T.; Arrechea, P. L. Simple and Efficient Synthesis of Functionalized Cyclic Carbonate Monomers Using Carbon Dioxide. *ACS Macro Lett.* **2022**, *11* (3), 368–375. <https://doi.org/10.1021/acsmacrolett.2c00060>.
- (50) *ibm/MoLFormer-XL-both-10pct · Hugging Face*.
<https://huggingface.co/ibm/MoLFormer-XL-both-10pct> (accessed 2024-08-12).

Supplementary Information

Materials and Methods

Vector Database Setup. All SMILES embeddings were computed using the *ibm/MoLFormer-XL-both-10pct* model available through HuggingFace using canonicalized SMILES (with the exception of the USPTO dataset, which was used as is).⁵⁰ For the example queries in Figures 1-4, the vector embeddings for each compound were L2 normalized prior to insertion into a Milvus lite vector database using an HNSW index and the L2 distance as the metric. For the multimodal examples (Fig. 5) SMILES embeddings were not L2 normalized and used in a Milvus standalone vector database using IVF_FLAT index and the L2 distance metric. For spectra containing more than one identifiable compound, including the NMR solvent, their corresponding embeddings were averaged prior to insertion. Image embeddings were computed using OpenCLIP via the Lanchain library. The model used was *ViT-g-14* with the *laion2b_s34b_b88k* checkpoint. Image embeddings were stored in a separate Milvus collection, using an IVF_FLAT index and L2 distance metric, and cross-referenced with their corresponding compound embeddings.

Similarity Metrics. For small molecule and polymer example queries, similarity metrics were computed on the basis of both the MoLFormer embeddings and molecular fingerprints computed using RDKit. Cosine similarity was computed by subtracting the cosine distance between the query and result embeddings (measured using the SciPy library) from 1. Euclidean similarity (E_s) was computed by the following equation:

$$E_s = 1 / (1 + E_d) \tag{1}$$

Where E_d is the Euclidean distance between the query and result embeddings. Tanimoto and Dice similarities were computed using the corresponding query and result Morgan fingerprints with a radius of 2 and a dimension of 2048. RDKit similarity was computed using the built-in RDKit fingerprints of the query and compound. MACCS similarity was computed using the MACCS Keys fingerprints of the query and the compound using the RDKit package.

Language Agent Network. As noted in the main text, the multi-agent framework was assembled using the Langgraph library. The supervisor agent utilized *GPT-4o mini* model while other agents used either *llava 7b* or *llama3.1 8b* models. All Milvus collections were instantiated as separate vector stores with customized embedding functions with either MoLFormer or OpenCLIP, prior to connection with LLM agents as retrievers. Full code for agent network will be released in both subsequent drafts of preprint and final publication.